David Forster, Fabian Kannenberg, Malte von Scheven, Achim Menges, Manfred Bischoff

Design and Optimization of Beam and Truss Structures Using Alternative Performance Indicators Based on the Redundancy Matrix

Abstract: In structural optimization processes, a common goal is to limit deflections or stresses through topological changes, shape adaption or cross-sectional adjustments. Beyond these well-established performance indicators, alternative measures for the assessment of structures based on the redundancy matrix can be used in the design and optimization process. This contribution shows the extension of the redundancy calculation to three-dimensional beam structures in detail. Using the concept of redundancy for the design of structures, one goal is to homogeneously distribute redundancy within a structure in order to make an overall collapse due to failure of individual elements less likely. Furthermore, the sensitivity towards imperfections is quantified by the redundancy matrix, offering the opportunity to design connections of substructures, such that no constraint forces are introduced during the assembly process. Those two concepts are showcased exemplarily within this contribution. The method is embedded into a computational co-design framework, which allows for quick, interactive feedback on design changes to strengthen the interplay between the design and engineering process.

Keywords: structural assessment, redundancy matrix, structural optimization

1 Introduction

The shortage of raw materials and the increasing necessity of creating a built environment for a growing population implies huge responsibility for architects, engineers and all other disciplines of the building sector. A well-known way to tackle the challenge of using less material in the design of structures comes with structural optimization. A well-established concept is to use the mass of the structure as the objective function to be minimized with side constraints like keeping displacements and stresses within defined limits (Haftka et al. 1990). This implies that the structure is analyzed with defined load cases which yield the calculation of stresses and deformations. In addition to the linear analyses, especially for slender structures, geometrically nonlinear effects like buckling are important to consider in the assessment of structures. Besides, an ultimate load analysis is commonly used to define the load bearing capacity of a structure. In contrast to these well-established approaches to structural assessment,

https://doi.org/10.1515/9783111162683-034

the present contribution uses alternative performance indicators to analyze structures and formulate design requirements. Those indicators are based on the redundancy matrix, first described by Bahndorf (1991). This concept is by no means replacing the above-mentioned methods, but rather complements the options. The redundancy matrix quantifies the distribution of the statical indeterminacy in the structure and by this offers the possibility to assess the structure's robustness and its sensitivity towards imperfections and is furthermore used in the field of adaptive structures (Geiger et al. 2020). We investigate the application of alternative performance indicators in the context of co-design, described by Knippers et al. (2021), meaning that the methods aim to be used integratively by multiple disciplines in the building sector, e. g. manufacturing alongside the classical ones like design and engineering. In that context, we show an example of using coreless filament wound (CFW) structures (Gil Pérez et al. 2022). Coreless filament winding is a manufacturing process that enables the fabrication of highly differentiated, lightweight, resource-effective, and high-performing building components and its application has been demonstrated for long-span and multi-story building systems (Menges et al. 2022). A CFW component is additively manufactured by freely spanning fiber rovings between anchor points, the resulting fiber net itself can form e. g. lattice components (Duque Estrada et al. 2021). CFW structures represent a particularly interesting application for alternative performance indicators since they are sensitive to imperfections and the redundancy distribution can be examined across multiple levels of detail.

Within this contribution, in Sec. 2 we recap the equations to calculate the redundancy matrix and showcase the details with a simple three-dimensional beam example. The optimization details and the integration of the design aspect are also covered in this chapter. Section 3 shows three different case studies. The first one deals with the assembly process, whereas the other two examples point toward a robust structural design in a spatial frame and a discrete gridshell structure. Section 4 summarizes the work and indicates possible future applications of the presented method.

2 Methodology

2.1 Redundancy matrices and statical indeterminacy

The derivation of the redundancy matrix will first be described in matrix notation for plane truss structures and then extended to three-dimensional beam structures. For a complete step-by-step derivation, the reader is referred to Scheven et al. (2021). In plane truss structures, the only deformation mode is the normal elongation.

The relation between external forces $\mathbf{F}_{\text{ext}}$ and internal forces $\mathbf{N}$ can be written as

$$\mathbf{A}^{\mathrm{T}}\mathbf{N} = \mathbf{F}_{\text{ext}}, \tag{1}$$

$\mathbf{A}^{\mathrm{T}}$ being the equilibrium matrix, capturing the topological and geometrical information of the discrete truss structure, and its transpose $\mathbf{A}$ being the compatibility matrix. Using the matrix $\mathbf{C}$, which includes each individual member stiffness on the main diagonal, the relation between internal forces and elastic elongations $\Delta\mathbf{l}_{\mathrm{el}}$ can be stated as follows:

$$\mathbf{N} = \mathbf{C}\Delta\mathbf{l}_{\mathrm{el}}. \tag{2}$$

The elastic elongations are calculated as the difference between the total elongation $\Delta\mathbf{l}$ and an initial, prescribed elongation $\Delta\mathbf{l}_0$. Initial prescribed elongations can be imagined as a member being imperfectly manufactured and therefore squeezed into the system with a certain force. The remaining necessary relation between total elongations and nodal displacements $\mathbf{d}$ reads:

$$\Delta\mathbf{l} = \mathbf{A}\mathbf{d}. \tag{3}$$

Equations (1) to (3) are used to solve for the unknown nodal displacements $\mathbf{d}$, neglecting external loads $\mathbf{F}_{\mathrm{ext}}$, leading to the desired load-independent measure. The redundancy matrix is then defined as the map between initial and elastic elongations:

$$\Delta\mathbf{l}_{\mathrm{el}} = \Delta\mathbf{l} - \Delta\mathbf{l}_0 = -\mathbf{R}\Delta\mathbf{l}_0 \qquad \mathbf{R} = \mathbf{1} - \mathbf{A}(\mathbf{A}^{\mathrm{T}}\mathbf{C}\mathbf{A})^{-1}(\mathbf{A}^{\mathrm{T}}\mathbf{C}). \tag{4}$$

It can be seen in eq. (4), that the redundancy distribution is independent of external loads and therefore a property of the structure only described by topology, shape, stiffness of the members and the support conditions. The main diagonal entries describe the constraint that is introduced on each individual member by the surrounding structure and quantify it with values between zero and one for truss structures.

The redundancy matrix can be used to quantify the distribution of the statical indeterminacy n_s within a structure. Classical formulas, see e. g. Maxwell (1864), describe the degree of statical indeterminacy as an integer number for the whole structure:

$$n_s = n_e - (2n_n - n_c). \tag{5}$$

Within this formula, n_e describes the number of elements, n_n is the number of nodes and n_c captures the number of fixed displacement degrees of freedom. Formally, the degree of statical indeterminacy describes the missing number of equilibrium equations that are necessary to calculate all internal forces of a structural system. In contrast to this consideration as an integer number, the redundancy matrix shows the spatial distribution of the statical indeterminacy within a structure on its main diagonal. The degree of statical indeterminacy can be calculated as the trace of the redundancy matrix:

$$n_s = \mathrm{tr}(\mathbf{R}). \tag{6}$$

If the redundancy of an element equals one, this element does not contribute to the load transfer of the system and can be removed without any impact on the load-bearing behavior of the system. If the redundancy of an element is zero, the element must not be removed because a deletion would produce at least a kinematic substructure and

therefore structural failure. Elements with zero redundancy are indispensable for the load transfer.

The extension to two-dimensional beam structures can be reviewed in detail in von Scheven et al. (2021), practical examples are already mentioned in Ströbel (1995). In contrast to trusses, for three-dimensional beams, six deformation modes are present. An eigenvalue decomposition of the element stiffness matrix of a three-dimensional beam element leads to a consistent description of the matrices **A** and **C**. The eigenvalues $\boldsymbol{\lambda}$ and eigenvectors $\boldsymbol{\phi}$ that are used to form those two matrices read as follows:

$$\boldsymbol{\lambda} = \begin{bmatrix} \frac{EA}{L} & 0 & 0 & 0 & 0 & 0 \\ 0 & \frac{3EI_z}{L} & 0 & 0 & 0 & 0 \\ 0 & 0 & \frac{3EI_y}{L} & 0 & 0 & 0 \\ 0 & 0 & 0 & \frac{GI_T}{L} & 0 & 0 \\ 0 & 0 & 0 & 0 & \frac{EI_y}{L} & 0 \\ 0 & 0 & 0 & 0 & 0 & \frac{EI_z}{L} \end{bmatrix} \quad \boldsymbol{\phi} = \begin{bmatrix} -1 & 0 & 0 & 0 & 0 & 0 \\ 0 & \frac{2}{L} & 0 & 0 & 0 & 0 \\ 0 & 0 & -\frac{2}{L} & 0 & 0 & 0 \\ 0 & 0 & 0 & -1 & 0 & 0 \\ 0 & 0 & 1 & 0 & -1 & 0 \\ 0 & 1 & 0 & 0 & 0 & -1 \\ 1 & 0 & 0 & 0 & 0 & 0 \\ 0 & -\frac{2}{L} & 0 & 0 & 0 & 0 \\ 0 & 0 & \frac{2}{L} & 0 & 0 & 0 \\ 0 & 0 & 0 & 1 & 0 & 0 \\ 0 & 0 & 1 & 0 & 1 & 0 \\ 0 & 1 & 0 & 0 & 0 & 1 \end{bmatrix}.$$

The redundancy matrix for three-dimensional beams has six rows and six columns per element, as opposed to one single row and column for truss systems. The individual contributions of the deformation modes to the redundancy are ordered in the same way as in the matrix above. The first entry refers to the elongation mode, the second and third entries refer to the coupled bending and shear modes in local y- and local z-direction respectively. The fourth eigenvector represents the torsional mode and the last two represent the pure bending modes.

Figure 1 shows a three-dimensional structure, consisting of an angled cantilever with an additional support in global Z-direction at the far end. The degree of statical indeterminacy is one. The respective redundancy matrix

$$\mathbf{R} = \begin{bmatrix} 0.0013 & 0.0 & 0.0 & 0.0 & -0.0013 & -0.0013 & 0.0 & 0.0 & 0.0009 & 0.0 & -0.0009 & 0.0 \\ 0.0 & 0.0 & 0.0 & 0.0 & 0.0 & 0.0 & 0.0 & 0.0 & 0.0 & 0.0 & 0.0 & 0.0 \\ 0.0 & 0.0 & 0.0 & 0.0 & 0.0 & 0.0 & 0.0 & 0.0 & 0.0 & 0.0 & 0.0 & 0.0 \\ 0.0 & 0.0 & 0.0 & 0.0 & 0.0 & 0.0 & 0.0 & 0.0 & 0.0 & 0.0 & 0.0 & 0.0 \\ -0.3394 & 0.0 & 0.0 & 0.0 & 0.3394 & 0.3394 & 0.0 & 0.0 & -0.2399 & 0.0 & 0.2399 & 0.0 \\ -0.3394 & 0.0 & 0.0 & 0.0 & 0.3394 & 0.3394 & 0.0 & 0.0 & -0.2399 & 0.0 & 0.2399 & 0.0 \\ 0.0 & 0.0 & 0.0 & 0.0 & 0.0 & 0.0 & 0.0 & 0.0 & 0.0 & 0.0 & 0.0 & 0.0 \\ 0.0 & 0.0 & 0.0 & 0.0 & 0.0 & 0.0 & 0.0 & 0.0 & 0.0 & 0.0 & 0.0 & 0.0 \\ 0.1131 & 0.0 & 0.0 & 0.0 & -0.1131 & -0.1131 & 0.0 & 0.0 & 0.0799 & 0.0 & -0.0799 & 0.0 \\ 0.0 & 0.0 & 0.0 & 0.0 & 0.0 & 0.0 & 0.0 & 0.0 & 0.0 & 0.0 & 0.0 & 0.0 \\ -0.3394 & 0.0 & 0.0 & 0.0 & 0.3394 & 0.3394 & 0.0 & 0.0 & -0.2399 & 0.0 & 0.2399 & 0.0 \\ 0.0 & 0.0 & 0.0 & 0.0 & 0.0 & 0.0 & 0.0 & 0.0 & 0.0 & 0.0 & 0.0 & 0.0 \end{bmatrix}$$

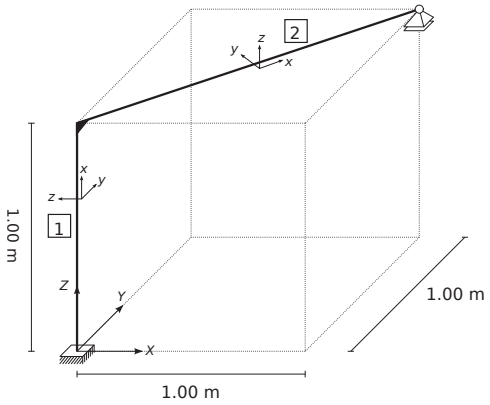

$E = 2.1 \cdot 10^8$ kN/m^2

Square hollow section:

$A = 30.4 \cdot 10^{-3}$ m^2

$I = 1.202 \cdot 10^{-5}$ m^4

Fig. 1: Three-dimensional cantilever with additional support.

shows that the numbers on the main diagonal sum up to one as described before (deviation due to rounding). The contribution of the torsional mode of element 1 is zero. The respective entry in the redundancy matrix can be found in the fourth column in the fourth row. This means that a prescribed torsion of the element is not constrained by the surrounding structure, since the additional support at the far end only fixes displacements in the global Z-direction.

2.2 Optimization using redundancy matrices

Structural optimization can basically be divided into three sub-categories, namely topology optimization, shape optimization and cross-sectional optimization, see Ramm et al. (1998). With regards to truss or beam structures, topology optimization answers the question of which node is connected to which node. Shape optimization defines the spatial coordinates of the nodes and cross-sectional optimization adjusts for example the thickness of a section. Using the distribution of statical indeterminacy as the objective function, changes within those categories offer the possibility to modify $\mathbf{C}$ and $\mathbf{A}$ in eq. (4) and thus redistribution of statical indeterminacy within the structure can be performed. In this work, we present an example using shape optimization; the design variables are denoted as $\mathbf{s}_1$. In a second example, the thickness of the cross-section is varied within a cross-sectional optimization. The design variables are defined as $\mathbf{s}_2$ and a similar optimization can be executed. The results are shown in Sec. 3.2, the

optimization problem is defined as:

$$\min_{\mathbf{s}} f(\mathbf{s}), \quad f(\mathbf{s}) = R_{\max} - R_{\min}, \quad \mathbf{s}_1 = \begin{bmatrix} x_1 \\ \vdots \\ x_n \\ y_1 \\ \vdots \\ y_n \\ z_1 \\ \vdots \\ z_n \end{bmatrix}, \; \mathbf{s}_2 = \begin{bmatrix} t_1 \\ \vdots \\ t_n \end{bmatrix}, \tag{7}$$

$R_{\max}$ being the maximum value of the redundancy of all elements and $R_{\min}$ being the minimum value. The optimum is obtained in MATLAB with the sequential quadratic programming (SQP) implementation (Nocedal and Wright 2006).

There exist already applications, where the redundancy distribution is used in the context of designing structures. In Wagner et al. (2018), the redundancy matrix is used in the design of adaptive structures, Kou et al. (2017) show the application in the context of robustness.

In Ströbel (1995), it is stated that the redundancy should be distributed homogeneously within a structure in order to prevent the collapse of the structure or of substructures in case of failure of specific elements, which is obtained with the optimization as stated in eq. (7). In case that a genuinely homogeneous redundancy distribution is achievable, the redundancy fraction of each element can be calculated by the ratio between the degree of statical indeterminacy and the number of elements. Since this might not always be possible, it is necessary to minimize the range and not just maximize the minimal value $R_{\min}$. For a two-dimensional frame, depending on the ratio between the bending stiffness and the normal stiffness, the different redundancy distributions reflect the importance of the elongation and the bending action in the load transfer, see von Scheven et al. (2021). For a rather homogeneous redundancy distribution, bending and elongation are of similar importance. As seen above, the total degree of statical indeterminacy gives only little insight into the load-bearing behavior. In order to design robust structures, the spatial distribution is of central importance.

Another aspect, where the distribution of statical indeterminacy can be used, is the assembly process. Regarding on-site structural assembly of pre-fabricated modules by connecting them with additional elements, it is desirable if the system can compensate for manufacturing inaccuracies. For truss systems, only imperfections in length are relevant. In a scenario, where substructures are to be connected, the optimal assembly sequence would include the additional elements in such a way that little to no constraint is introduced and imperfections can be compensated through displacements of the

already assembled structure. In an optimal case, the additional elements would have zero redundancy.

2.3 Design integration

Interactive design methods require fast feedback to inform the designers and guide them in their decision-making process. Feedback on the redundancy distribution is particularly useful for topology exploration of the global design, independent of specific load cases. The calculation of the redundancy matrix can be made relatively fast (Tkachuk et al. 2023), making it suitable for quick feedback and interactive design methods such as agent-based modeling and simulation (Stieler et al. 2022). This has been investigated by Maierhofer and Menges (2019) in the context of adaptive truss structures. The codebase for calculating the redundancy distribution for truss and beam structures has been implemented as a `C#` library that can be referenced in CAD environments such as Rhino/Grasshopper or interactive platforms like Unity.

2.4 Application context

In the context of CFW, the method can be applied across different scales. Firstly, on the global design level, allowing for investigation of the overall topology and shape of a structure. Secondly, we can examine the redundancy distribution of CFW building elements on the component level. The fiber net, a result of the interaction of the free-spanning fiber rovings (see Fig. 2), can be conceptualized as a beam structure and the redundancy contribution of each fiber segment can be computed (see Fig. 3). In contrast to the global design, optimization of the fiber net is non-trivial, as the fiber net results from the interaction of the sequentially laid fiber rovings and the final form, the number of nodes and the topology of the structure emerge only at the end (Menges et al. 2022). Therefore, the optimization of the fiber net needs to interface with a simulation of the fiber-fiber interaction. As part of the co-design framework for CFW building systems, the calculation can take cross-section input from other domains via the fiber data object model (Gil Pérez et al. 2022). Figure 3 shows the simulated fiber-fiber interaction and the resulting fiber net in the winding frame in the left. The middle plot shows the redundancy distribution in color scheme with preliminary assumptions that include constant cross-sections. The plot on the right shows the redundancy distribution in color scheme with the measured cross-sections from the physical testing specimen. Significant differences are visible, underlining the sensitivity of the manufacturing process.

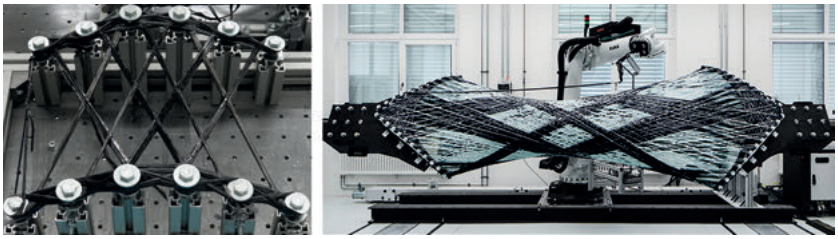

Fig. 2: Examples of coreless filament wound fiber nets: small-scale mechanical testing specimen (left), full-scale building component (right), © ICD/ITKE University of Stuttgart.

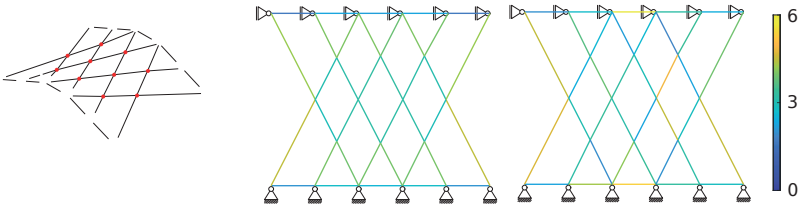

Fig. 3: Result of the winding sequence shown in the winding frame (left). Redundancy distribution with constant cross-sections (middle). Redundancy distribution with cross-sections measured from specimen S3-0 (right); data taken from Gil Pérez et al. (2023). Color spectrum for the redundancy distributions on the right.

3 Numerical examples and discussion

3.1 Specific redundancy for optimized assembly process

As described in Sec. 2.2, during the assembly process it can be of importance that only little constraint forces are introduced. Figure 4 a) shows two pre-fabricated parts of a truss bridge, both of which have a degree of statical indeterminacy of $n_s = 1$. Those pre-fabricated parts will be connected by three elements on-site and the vertical supports at the inner part of the final structure as well as the horizontal support at the right outer node are to be removed during the assembly process. The assembly sequence is shown from a) to d). The first additional member is shown in b). At the same time, the aforementioned horizontal support is removed. The additional member has zero redundancy. The second member, connecting the two parts diagonally makes one vertical support obsolete. In the final step, shown in d), another horizontal member is added and no more supports remain in the inner part of the structure. Throughout the assembly process, all members that were added have zero redundancy. Thus, the assembly process can fully compensate for possible manufacturing imperfections of the connecting elements and no constraint forces are introduced. It should be noted, that every additional member thereafter would raise the overall degree of statical

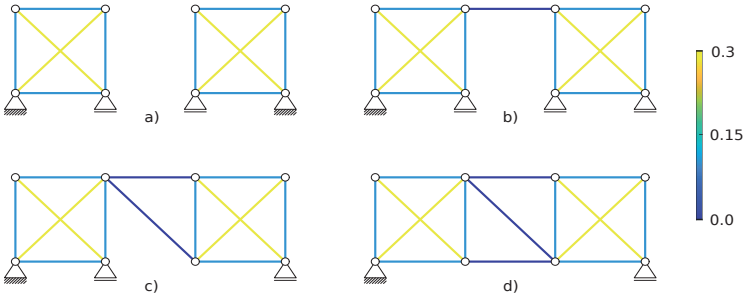

Fig. 4: Assembly sequence from configuration a) to d) with zero constraint forces introduced during the process; color spectrum showing the redundancy distribution.

indeterminacy and therefore, constraint forces would be introduced in case of imperfect manufacturing.

This simple two-dimensional truss example showcases, that it is possible to account for imperfections in the assembly and manufacturing process through knowledge of the spatial distribution of the statical indeterminacy of a system.

3.2 Homogeneous redundancy distribution

The first example is a spatial frame structure, shown in Fig. 5. The structure consists of 59 elements with a constant cross-section and a length of 5 m per element. The connections of the elements are rigid and at the four bottom corner nodes, the displacements are fixed by supports. The initial redundancy distribution can be seen in Fig. 5 on the left, with a range of $R_{\text{max,init}} - R_{\text{min,init}} = 1.05$. An optimization is performed, using the spatial coordinates of the nodes as the design variables, see eq. (7), such that the nodes can change position by 3.0 m in each spatial direction. Furthermore, the structure was kept to be symmetric during the optimization. One can see on the right that the redundancies are distributed homogeneously within the structure after changing the nodal positions, the final values only ranging negligibly from $R_{\text{max,opt}} = 3.154$ to $R_{\text{min,opt}} = 3.149$. In accordance to Sec. 2.2, the small range of the redundancy distribution reflects that the effect of removing any single element is of similar influence rather than one element having a large effect on the load-bearing behavior when being removed.

As a second example, the triangulated base geometry of the segmented timber shell from the Landesgartenschau Exhibition Hall (Krieg et al. 2015) is used in order to test the method on a geometrically more complex structure. The center points of the individual timber plates are connected by lines. By this, we generate a large-scale discrete gridshell to test the presented method without referring to the original timber shell and its planar plate segments. The structure consists of 243 nodes that are connected by 638 elements, see Fig. 6. The structure is supported on 34 nodes and has two openings that are curved. At the supports, only the displacements are set to zero. Using the cross-sectional

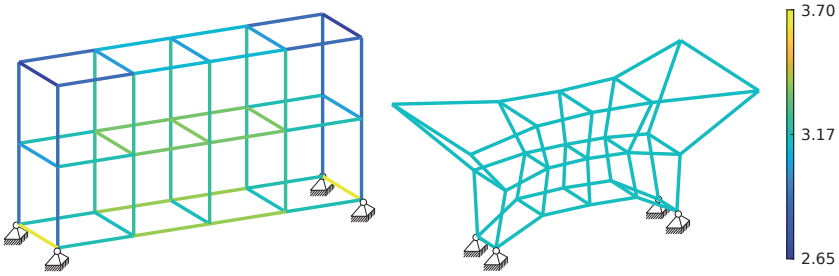

Fig. 5: Redundancy distribution of initial configuration (left) and optimized configuration with new nodal positions (right), geometry of a spatial frame structure shown in color spectrum.

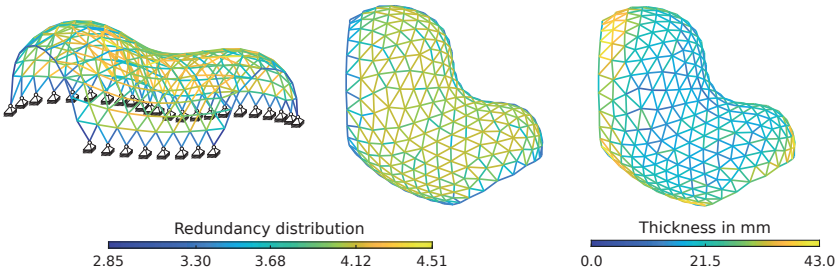

Fig. 6: Redundancy distribution of initial configuration (left) and optimized configuration with new cross-sectional thickness (middle) in color spectrum. Cross-sectional thicknesses in color spectrum (right).

thickness as the design variable, see $\mathbf{s}_2$ in eq. (7), the initial thickness was set to 10 mm using a hollow circular section with 244.5 mm diameter. The goal is to homogenize the redundancy as much as possible within the structure. As it is described in Sec. 2.2, the distribution of the redundancy in the overall structure is a measure of its robustness. This means that in areas with high redundancy fractions, many alternative load paths are available for the load transfer. In Fig. 6 on the left, one can see that the elements that are connected to the supports as well as the elements that build the curved openings are the ones that have the lowest redundancy fraction. The color spectrum ranges from the minimum to the maximum redundancy value of the initial configuration, which is $R_{\text{max,init}} - R_{\text{min,init}} = 1.66$.

In Fig. 6, the optimized redundancy distribution is shown in the middle. The maximum and minimum numbers are closer compared to the initial configuration with equal cross-sections for all elements. The range in the optimized configuration is $R_{\text{max,opt}} - R_{\text{min,opt}} = 0.82$, with the values shown in the color spectrum. On the right, the thickness of the cross-sections is shown in the colorspectrum. One can see that in order to homogenize the redundancy within the structure, the thickness of the cross-sections in the outer parts of the structure is increased, whereas the elements with smaller thickness are present in the inner part of the structure.

4 Conclusion and outlook

The redundancy matrix captures information about the spatial distribution of the degree of statical indeterminacy within a structure. This information can be used to define different goals for the design process of structures. Using the information about statical indeterminacy in the assembly process, the first example showed that constraint-free sequences can be determined. The application in the design of robust structures was showcased in the second and third example. To overcome the shortcomings of the restriction to linear calculations, an extension to non-linear analyses and to ultimate load analyses are subject to present research. Future work includes consideration of additional side constraints such as manufacturing requirements, especially in the context of CFW fiber nets. As the six modes of contribution for three-dimensional beams pose a challenge for visualization, the previously developed visual analytics method for fiber nets (Abdelaal et al. 2022) could be extended to include information about the redundancy distribution.

The presented method is universally applicable to truss and beam structures and has been demonstrated on a variety of geometries. It opens a field of alternative measures for structural assessment, beyond well-established parameters like e. g. stresses and displacements, that are applicable to various building systems across scales.

Acknowledgements

This research was supported by the Deutsche Forschungsgemeinschaft (DFG; German Research Foundation) under Germany's Excellence Strategy – EXC 2120/1 – 390831618. The authors would like to thank Mathias Maierhofer for sharing the codebase of the initial truss implementation and student assistant Henrik Jakob for his support. The fiber net simulation was developed by Valentin Noah Hartmann at IPVS-MLR, University of Stuttgart.

References

Abdelaal, M., F. Amtsberg, M. Becher, R. D. Estrada, F. Kannenberg, A. S. Calepso, H. J. Wagner, G. Reina, M. Sedlmair, A. Menges, and D. Weiskopf (2022). Visualization for architecture, engineering, and construction: Shaping the future of our built world. *IEEE Computer Graphics and Applications 42* (2), 10–20.

Bahndorf, J. (1991). *Zur Systematisierung der Seilnetzberechnung und zur Optimierung von Seilnetzen.* Ph. D. thesis, Universität Stuttgart, Stuttgart.

Duque Estrada, R., F. Kannenberg, H. J. Wagner, M. Yablonina, and A. Menges (2021). Integrative design methods for spatial winding. In O. Baverel, C. Douthe, R. Mesnil, C. Mueller, H. Pottmann, and T. Tachi (Eds.), *Advances in Architectural Geometry 2020,* Paris, pp. 286–305. Presses des Ponts.

Geiger, F., J. Gade, M. von Scheven, and M. Bischoff (2020). Anwendung der Redundanzmatrix bei der Bewertung adaptiver Strukturen. In B. Oesterle, M. von Scheven, and M. Bischoff (Eds.), *Baustatik – Baupraxis 14,* pp. 119–28. Institute for Structural Mechanics, University of Stuttgart.

Gil Pérez, M., C. Zechmeister, F. Kannenberg, P. Mindermann, L. Balangé, Y. Guo, S. Hügle, A. Gienger, D. Forster, M. Bischoff, C. Tarín, P. Middendorf, V. Schwieger, G. Gresser, A. Menges, and J. Knippers (2022, April). Computational co-design framework for coreless wound fibre-polymer composite structures. *Journal of Computational Design and Engineering 9* (2), 310–29.

Gil Pérez, M., C. Zechmeister, F. Kannenberg, P. Mindermann, L. Balangé, Y. Guo, S. Hügle, A. Gienger, D. Forster, M. Bischoff, C. Tarín, P. Middendorf, V. Schwieger, G. T. Gresser, A. Menges, and J. Knippers (2023). Object model data sets of the case study specimens for the computational co-design framework for coreless wound fibre-polymer composite structures.

Haftka, R. T., Z. Gürdal, and M. P. Kamat (1990). *Elements of structural optimization* (Second revised edition ed.). Dordrecht: Springer Netherlands. OCLC: 851381183.

Knippers, J., C. Kropp, A. Menges, O. Sawodny, and D. Weiskopf (2021, September). Integrative computational design and construction: Rethinking architecture digitally. *Civil Engineering Design* 3 (4), 123–35.

Kou, X., L. Li, Y. Zhou, and J. Song (2017). Redundancy Component Matrix and Structural Robustness. *International Journal of Civil and Environmental Engineering 11* (8), 1155–60.

Krieg, O. D., T. Schwinn, A. Menges, J.-M. Li, J. Knippers, A. Schmitt, and V. Schwieger (2015). Biomimetic lightweight timber plate shells: Computational integration of robotic fabrication, architectural geometry and structural design. In P. Block, J. Knippers, N. J. Mitra, and W. Wang (Eds.), *Advances in Architectural Geometry 2014,* Cham, pp. 109–25. Springer International Publishing.

Maierhofer, M. and A. Menges (2019). Towards integrative design processes and computational design tools for the design space exploration of adaptive architectural structures. In *International Conference on Emerging Technologies in Architectural Design (ICETAD2019),* Toronto, Canada.

Maxwell, J. C. (1864, April). On the calculation of the equilibrium and stiffness of frames. *The London, Edinburgh, and Dublin Philosophical Magazine and Journal of Science 27* (182), 294–9.

Menges, A., F. Kannenberg, and C. Zechmeister (2022). Computational co-design of fibrous architecture. *Architectural Intelligence 1* (1), 6.

Nocedal, J. and S. J. Wright (2006). *Numerical optimization* (2nd ed.). Springer series in operations research and financial engineering. New York: Springer.

Ramm, E., K. Maute, and S. Schwarz (1998). Conceptual design by structural optimization. In *Proceedings of EURO-C 1998,* R. de Borst, N. Bicanic, H. Mang, G. Meschke (eds), Badgastein, Austria, March 31 - April 3, 1998, Balkema, Rotterdam, pp. 879–96.

Stieler, D., T. Schwinn, S. Leder, M. Maierhofer, F. Kannenberg, and A. Menges (2022). Agent-based modeling and simulation in architecture. *Automation in Construction* 141, 104426.

Ströbel, D. (1995). *Die Anwendung der Ausgleichungsrechnung auf elastomechanische Systeme.* Ph. D. thesis, Universität Stuttgart, Stuttgart.

Tkachuk, A., T. Krake, J. Gade, and M. von Scheven (2023). Efficient Computation of Redundancy Matrices for Moderately Redundant Truss and Frame Structures. DOI: 10.48550/arXiv.2303.03945

von Scheven, M., E. Ramm, and M. Bischoff (2021). Quantification of the redundancy distribution in truss and beam structures. *International Journal of Solids and Structures 213,* 41–49.

Wagner, J. L., J. Gade, M. Heidingsfeld, F. Geiger, M. von Scheven, M. Böhm, M. Bischoff, and O. Sawodny (2018, August). On steady-state disturbance compensability for actuator placement in adaptive structures. *at - Automatisierungstechnik 66* (8), 591–603.